A Novel One-To-One Multiscale Approach to Computational Mechanics of Materials

Dubravka Mijuca[*] and Sreten Mastilović [**]
[*]Department of Mechanics, Faculty of Mathematics, University of Belgrade
[**]Center for Multidisciplinary Studies, University of Belgrade
E-mail: dmijuca@matf.bg ac.yu

Abstract – A novel approach in computational modelling on scales ranging from the atomistic, through the microscopic, up to the continuum is presented. It is shown that present multiscale numerical approach, based on direct linking (that is one-to-one correspondence between molecular dynamics on atomistic scale and primal-mixed finite element scheme on macroscale), is reliable and efficient. It is shown that seamless semi-coupling between length scales is achieved, in spite of two main challenges, the computational complexity of coupled simulations via the coarse-graining approach and, secondly, the inherent difficulty in dealing with system evolution stemming from time scaling, which does not permit coarse graining over temporal events. Presently, the original primal-mixed finite element method is used, to describe the nonlinear deformation behavior of materials at the local macroscopic scales, that is, on continuum-mechanics-based framework, while molecular dynamics and embedded-atom interatomic potential is used on atomic scale. The reliability of present approach relies on robustness of primal-mixed finite element scheme, which is insensitive to distortion of the finite element in the mesh and high ratio of its maximal and minimal axial dimensions.

Key words: *continuum mechanics, multifield finite element method, multiscale, molecular dynamics, direct linking scheme*

1. INTRODUCTION

Despite the fact that the continuum mechanics (including the computational techniques such as the finite element method) have yielded many useful results and continue to be the workhorse of applied mechanics - notably in industry, the continuum viewpoint of the fracture is inherently limited to the extent that it neglects the atomistic structure of solids. Accordingly, in fracture, "as in any thermodynamic process, the final answers must be sought at the atomistic or molecular level" [1]. On the other hand, in the analysis of the nanoscale phenomena it is frequently necessary to consider models whose size exceeds the computational tractability of the molecular mechanics with current computers. The conflicting requirements for the computational expediency and the capability of a model to capture salient features of a physical problem are often addressed by coupling of the length scales [2][11].

Although appropriate for most of the problems in modern engineering structural assessment, continuum mechanics can not readily described certain heterogeneities linked to either the microstructure or the deformation (crack nucleation in fatigue, dislocation patterns, bifurcation phenomena, some non-local phenomena).

In design of large structures in the aerospace, deep marine or nuclear industries, the effects of ageing and environment on failure mechanisms cannot be left to conservative approaches. Namely, continuum mechanics (CM) can be used alone only if there is inherent assumption that material properties vary continuously throughout the solid. It is nowadays widely accepted that dual nature of the structure of matter, continuous when viewed at large length scales and discrete when viewed at an atomic scale, can be traced only by the multiscale materials modelling (MMM) approaches. Reliable numerical MMM approaches should harmonize continuum and atomistic analyses methods.

The presented molecular dynamics (MD) simulation, employs the embedded-atom method (EAM) [4]. It is limited to several thousands atoms because of the hardware limitations (PC Pentium IV on 2.4 GHz, 1GB RAM configuration), which is admittedly not even close to the current state-of-art MD capabilities of several hundred millions atoms. The interconnections between atoms are simulated by interatomic potential, understanding that it may not provide the desired physical accuracy for many real complex materials of interest. For example, reliable interatomic potentials are often not available for multielement materials and for systems containing interstitial or substitutional alloying impurities.

Nevertheless, proper choice of interatomic potential is of crucial importance in obtaining physically meaningful results. In general, there is a compromise between the potential rigorousness and the computational efficiency. For high computational efficiency, pair potentials, such as the Lennard-Jones potential are still often employed. These simple potentials have very few fitting parameters easily determined from crystal properties. On the other hand, this potential suffers from non-transferability. Since these potentials are fitted to only a few perfect crystal properties, their applicability in studying defects is by default questionable.

On a first sight, solving MD second-order ordinary differential equations for all the atoms in an ensemble may appear simplistic. Nevertheless, a physical simulation involves employment of appropriate boundary conditions, stress and temperature control to imitate physically meaningful thermodynamic ensembles, and proper selection of numerical integration scheme which should be both numerically stable, as well as computationally efficient.

Two types of boundary conditions often used between CM and MD domains are the flexible and direct linking scheme (for a detailed overview see [5]). The flexible boundary conditions, often referred to as the Green's-function boundary conditions, have been extended to three dimensions [6]. The flexible boundary conditions have some advantages over the direct linking scheme; however, Green's-function calculations are time-consuming, which limits applicability of the flexible boundary condition. In the present approach the *direct linking scheme* between MD and CM domains is adopted. As emphasized in [5], "once numerically robust and efficient, the direct linking scheme should be the most reliable and desirable boundary condition."

In addition to the above issues of numerical integration and boundary conditions, successful MD simulations rely on the appropriate control of thermodynamic variables such as temperature or pressure. Temperature is controlled through the kinetic energy or velocities of all atoms. For the sake of simplicity, it is assumed in the present study that temperature is uniform in space, and the Nose-Hoover thermostatting formalism (as presented in [12]) is adopted.

The computational thermo-mechanical CM analysis of solids is very important in nowadays engineering calculations. Nevertheless, there are issues of reliability, transition error, tensorial invariance, consistency error, introduction of the residual stresses, and introduction of the initial deformations, unwanted spurious oscillation of primal and dual variable fields, thermal stress calculation, no dimensional reduction, scale robustness, robustness of material properties, material interfaces, and presence of the thin inner or outer layers of materials, which must be addressed in order to have confidence in numerical results [3]. Usually some of these issues are possible to overlook and again obtain structural response with low verification and validation error.

However, when all of these issues are present in the same structure, the system analyst is facing the problem that no numerical procedure is capable of addressing in the satisfactory manner. As a simple and natural method of discretization, the finite element method based on extremal principles is not capable to deal with all of these issues also, contrary to the new semi-coupled primal-mixed finite element approach which is presently used.

Therefore, in the present paper two semi-coupled approaches for nano-scale and macro-scale analyses are used, which are both reliable computational schemes in their domains. The first author of the present paper is responsible for the CM analysis, while the second author is responsible for the MD analysis.

Bridging of two domains is performed utilizing the direct linking scheme connecting boundary atoms of MD domain to the boundary nodes of the finite element domain. Field variable of interest which is transferred from MD to CM domain is displacement. It should be noted, that success of present approach rely solely on robustness of CM primal-mixed scheme which is insensitive to distortion of the finite element in the mesh, that is, present three-dimensional HC8/27 finite elements may have extremely high ratio of its maximal axial dimensions and maintain its stability and robustness.

2. CONTINUUM MECHANICS METHOD

Presently, a three-dimensional thermo-mechanical multifield primal-mixed finite element method [3] is used, to describe the nonlinear deformation behavior of materials at the local macroscopic scales, that is, on CM-based framework. It is used for analysis of either isotropic or anisotropic materials, or almost incompressible materials, with or without (thermal barrier) coatings or bonds or abrupt material changes. Its unique properties are stress approximation by the continuous base functions, introduction of stress constraints as essential boundary conditions, and initial stress/strain field capability, residual stress implementation. The relevant hexahedral finite element HC8/27 satisfies mathematical convergence requirements, like consistency and stability, even when it is rigorously slandered, distorted or used for the nearly incompressible materials. In order to minimize accuracy error and enable introductions of displacement and stress constraints, the tensorial character of finite element equations is fully respected. Present finite element approach has four fundamental variables of interest, per which essential boundary conditions may be prescribed: displacement, stress, temperature, and heat flux.

In elasticity analysis present CM scheme can be written as the system of linear equations of order $n = n_u + n_t$, where n_u is the number of displacement degrees of freedom, while n_u is the number of stress degrees of freedom:

$$\begin{bmatrix} \mathbf{A}_{vv} & -\mathbf{D}_{vv} \\ -\mathbf{D}_{vv}^{\ T} & \mathbf{0} \end{bmatrix} \begin{bmatrix} \mathbf{t}_v \\ \mathbf{u}_v \end{bmatrix} = \begin{bmatrix} \mathbf{-A}_{vp} & \mathbf{D}_{vp} \\ \mathbf{D}_{pv}^{\ T} & \mathbf{0} \end{bmatrix} \begin{bmatrix} \mathbf{t}_p \\ \mathbf{u}_p \end{bmatrix} - \begin{bmatrix} 0 \\ \mathbf{f}_p + \mathbf{p}_p \end{bmatrix}. \quad (1)$$

In this expression, unknown (variable) and known (initial, prescribed) values of the stresses and displacements, denoted by the indices v and p respectively, are decomposed. The nodal stresses t^{Lst} and displacements u_{Kq} components are consecutively ordered in the column matrices $\mathbf{t}$ and $\mathbf{u}$ respectively. The homogeneous (zero) and nonhomogenous (nonzero) essential boundary conditions per displacements $\mathbf{u}_p$ and stresses $\mathbf{t}_p$ are introduced as contribution to the right-hand side of the expression (1).

The members of the matrices $\mathbf{A}$ and $\mathbf{D}$, of the column matrices $\mathbf{f}$ and $\mathbf{p}$ (discretized body and surface forces) in (2), are respectively:

$$\begin{aligned} A_{\Lambda uv\Gamma st} &= \sum_e \int_{\Omega_i} \Omega_\Lambda^N S_N g_{(\Lambda)u}^a g_{(\Lambda)v}^b A_{abcd} g_{(\Gamma)s}^c g_{(\Gamma)t}^d T_L \Omega_\Gamma^L d\Omega \\ D_{\Lambda uv}^{\Gamma q} &= \sum_e \int_{\Omega_e} \Omega_\Lambda^N S_N U_a^K \Omega_K^\Gamma g_{(\Lambda)u}^a \, g_{(\Lambda)v}^{(\Gamma)q} d\Omega \\ f^{\Lambda q} &= \sum_e \int_{\Omega_e} g_a^{(\Lambda)q} \Omega_M^\Lambda V^M \, f^a d\Omega \\ p^{\Lambda q} &= \sum_e \int_{\partial\Omega_{it}} g_a^{(\Lambda)q} \Omega_M^\Lambda V^M \, p^a d\partial\Omega \end{aligned} \quad (2)$$

By analogy with above finite element approach in elasticity [3], transient heat transfer finite element approach can be written as a system of linear equations of order $n = n_q + n_T$, where n_T is the number of temperature degrees of freedom, while n_q is the number of flux degrees of freedom, in matrix form at the current time t:

$$\begin{bmatrix} \mathrm{A}_{vv} & \mathrm{B}_{vv}{}^{T} \\ \mathrm{B}_{vv} & -\mathrm{D}_{vv} - \mathrm{S}_{vv} \end{bmatrix} \begin{bmatrix} \mathbf{q}_v \\ \mathrm{T}_v \end{bmatrix} = \begin{bmatrix} -\mathrm{A}_{vp} & -\mathrm{B}_{vp}{}^{T} \\ -\mathrm{B}_{vp} & \mathrm{D}_{vp} \end{bmatrix} \begin{bmatrix} \mathbf{q}_p \\ \mathrm{T}_p \end{bmatrix} + \begin{bmatrix} 0 & 0 \\ 0 & \mathrm{S}_{vp} \end{bmatrix} \begin{bmatrix} 0 \\ \mathrm{T}_p^{(t-1)} \end{bmatrix} + \begin{bmatrix} 0 \\ \mathrm{F}_p + \mathrm{H}_p - \mathrm{K}_p \end{bmatrix} + \begin{bmatrix} 0 \\ -\mathrm{L}_p^{(t-1)} \end{bmatrix} \tag{3}$$

In this expression, unknown (variable) and known (initial, prescribed) values of the fluxes and temperatures, denoted by the indices v and p respectively, are decomposed. The nodal flux (q^{pL}) and temperature (T^L) components are consecutively ordered in the column matrices $\mathbf{q}$ and T respectively.

The homogeneous and nonhomogenous essential boundary conditions per temperature T_p and heat flux $\boldsymbol{q}_p$ are introduced as contribution to the right-hand side of the expression (3). The members of the entry matrices A, B, D and S, and the column matrices F, H, K and L in (3), are respectively:

$$\begin{aligned}
A_{\Lambda p \Gamma r} &= \sum_e \int_{\Omega_e} \overset{(e)}{\Omega}{}^L_\Lambda \, g^a_{(L)p} V_L k^{-1}_{ab} g^b_{(M)r} V_M \, \overset{(e)}{\Omega}{}^M_\Gamma \, d\Omega_e; \\
B_{\Lambda p \Gamma} &= \sum_e \int_{\Omega_e} \overset{(e)}{\Omega}{}^L_\Lambda \, g^a_{(L)p} V_L P_{M,a} \, \overset{(e)}{\Omega}{}^M_\Gamma \, d\Omega_e \\
D_{\Lambda\Gamma} &= \sum_e \int_{\partial\Omega_{ce}} h_c \, \overset{(e)}{\Omega}{}^L_\Lambda \, P_L P_M \, \overset{(e)}{\Omega}{}^M_\Gamma \, \partial\Omega_{ce}; \\
F_\Gamma &= \sum_e \int_{\Omega_e} \overset{(e)}{\Omega}{}^M_\Gamma \, P_M \, f \, d\Omega_e \\
H_\Gamma &= \sum_e \int_{\partial\Omega_{he}} \overset{(e)}{\Omega}{}^M_\Gamma \, P_M h d\partial\Omega_{he}; \\
K_\Gamma &= \sum_e \int_{\partial\Omega_{ce}} \overset{(e)}{\Omega}{}^M_\Gamma \, P_M h_c T_0 d\partial\Omega_{ce} \\
S_{\Lambda\Gamma} &= \sum_e \int_{\Omega_e} \frac{\rho c}{\Delta t} \overset{(e)}{\Omega}{}^L_\Lambda \, P_L P_M \, \overset{(e)}{\Omega}{}^M_\Gamma \, d\Omega_e; \\
L_\Gamma &= \sum_e \int_{\Omega_e} \frac{\rho c}{\Delta t}{}^{n-1}T_{(M)} \, P_M \, \overset{(e)}{\Omega}{}^M_\Gamma \, d\Omega_e
\end{aligned} \tag{4}$$

2.1 RELIABILITY OF CM SCHEME

It is shown [3] that finite element scheme HC8/27 is reliable in every limit scenarios, such as thin solid body, almost incompressible material, highly distorted mesh. Therefore, we may say that success of the present scheme is due to the reliability of the present primal-mixed finite element approach, which satisfies all convergence criteria, such as robustness, solvability, consistency and stability [7].

3. MOLECULAR DYNAMICSS METHOD

The MD method relies on description of simultaneous motion and interaction of atoms (or molecules). The dynamic evolution of the system is governed by classical Newtonian mechanics, where for each atom i the equation of motion is given by

$$M_i \frac{d^2 R_i}{dt^2} = F_i = -\nabla_{R_i} \Phi, \tag{5}$$

which is derived from classical Hamiltonian of the system:

$$H = \sum \frac{M_i V_i^2}{2} + \Phi, \tag{6}$$

An atom of mass M_i moves as a rigid particle at the velocity V_i in the effective potential $\Phi(R_i)$ of other particles. The atomic force F_i is obtained as the negative gradient of the effective potential: $F_i = -\nabla_{R_i} \Phi$. Presently, the embedded-atom interatomic potential (see [11] for details) is used in calculations within the nearest-neighbor approximation.

The close-packed crystal lattice is used within the MD framework to model the atomistic domain of the solid structure. The embedded-atom potential has proven to be a good choice for simulations of plastic deformation of simple metals [4], as presently considered.

4. SEMI-COUPLING BETWEEN DM AND CM DOMAINS

The present bridging approach introduces a three-dimensional multiscale approach to thermo-mechanical analysis of a crystalline lattice with defects (the MD method), embedded in a large continuum domain (the finite element method). This approach has been arousing perennial interest in the research community since it offers advantage of deeper understanding of the underlining physical phenomena facilitated by the MD with the computational expediency of the finite element method; an appropriate computational technique is used for each scale.

At the interface between the two domains there is a direct kinematic coupling between atoms and nodes of the finite element mesh. The direct linking of atomistic and continuum regions [8] is presently adopted in three dimensions.

The field variable of interest, which is transferred from DM to CM domain, is displacement. Displacements of the boundary atoms are used as prescribed displacements for the finite element nodes on the boundary of the CM domain. Then, when displacement field of the CM domain is calculated, new boundary CM displacements are imposed as the new boundary conditions to the new MD analysis iteration, until the equilibrium is reached. It should be noted, that success of present approach rely solely on robustness of CM primal-mixed scheme which is insensitive to distortion of the finite element in the mesh, that is, present three-dimensional HC8/27 finite elements may have extremely high ratio of its maximal axial dimensions and maintain its stability and robustness.

The goal of the present approach is to offer a tool for studying the microscopic bases of many macroscale phenomena (including the subtle features of fracture), which opens pathway for structural engineering of materials on nanoscale and microscale

5. LARGE SCALE COMPUTATION

The present CM primal-mixed finite element approach produces has system matrix that is large, quadratic, symmetric, sparse, and indefinite. Therefore, the modified direct MA47 solution procedure, particular version of the Duff-Reid algorithm [9], which solves a sparse symmetric indefinite system of linear equations using multifrontal Gaussian elimination and makes a special effort to exploit the zero block from present saddle point problem, is presently used.

The scaling routine MC30 [9] is also used in order to increase robustness of the solution procedure in the case of geometrically multiscale analyses. The performance of the adjusted solution method is studied and compared with existing in-house sparse Gaussian elimination solver (SSGE). The numerical examples are calculated on the PC Pentium IV on 2.4 GHz, 1GB RAM configuration. The results obtained, confirmed the efficiency and reliability of the MA47 procedure.

6. NUMERICAL EXAMPLES

A first example is done by continuum mechanics HC8/27 approach to demonstrate its reliability even on submicron-scales.

The second example is a simulation of the quasi-static nano-indentation by using the described multiscale approach.

6.1 THERMAL BARRIER COATING

A hollow long steel shaft coated by a bond layer and a ceramic layer shown in Fig.1, is analyzed. Thermal conductivity of the steel and bond is $k = 25W/(mK)$, while thermal conductivity of the ceramics is taken to be $k = 1W/(mK)$. The outer radius of shaft is $r_0 = 0.1m$, and the inner radius of the shaft is $r_3 = 0.005m$. It is presently assumed that height of the shaft is $h = 0.1m$. Five model problems with decreasing thickness t of coating (bond and ceramic), varied from $10^{-2}m$ to $10^{-6}m$, are presently considered. The temperature boundary conditions are prescribed: on the inner surface temperature is $T_3 = 500^0C$, and on the outer surface $T_0 = 1000^0C$.

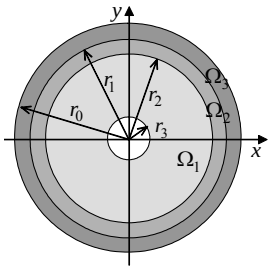

Fig.1. Thermal barrier coating model problem

The results obtained by present finite element configurations HC8/9 and HC20/21 are compared with results obtained by two-dimensional conventional boundary element approach (CBEM) and analytical (target) results, which are reported in [10]. One-eight segment of the cylinder is analyzed due to the symmetry of geometry and thermal loading.

All five model problems are discretized by only eight finite elements along circumference, and one finite element layer along height. The radial meshing is performed such that mesh is gradually refined toward coating. Approximate number of finite elements in the mesh for five models, from that one with thickest coating to that one with thinnest coating, is 120, 160, 192, 248, and 384, respectively. Non-dimensional temperature T_1/T_0 and radial heat flux component q_1/q_0, versus non-dimensional coating thickness $n = \log(r_0/t)$, are given in Fig.2.

From Fig.2, it can be seen that present approach has excellent agreement with analytical solution, while classical boundary element method exhibit spurious behavior. Therefore, it is shown that present approach can be an efficient tool for thermal barrier coating design. Execution times for all model problems, five model problems discretized by HC8/9 finite elements, and five model problems discretized with HC20/21, are in range from 0.3 to 25.7 seconds, respectively, on PC Pentium 1GB RAM, 2.4MHz. The same level of accuracy is obtained in the subsequent thermal stress analysis shown in Fig.3.

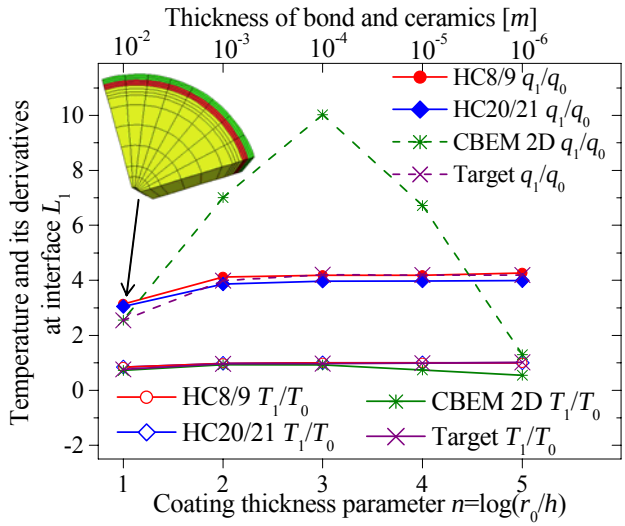

Fig.2. Coating model: Temperature and heat flux

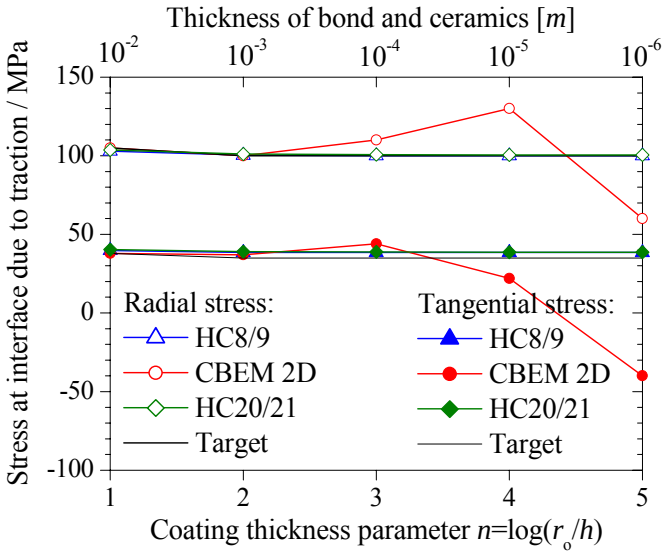

Fig.3. Coating model: Mechanical induced stress

6.2 NANO-IDENTATION

A model problem of the quasi-static nano-indentation shown in Fig.4 and 5, is considered. Namely, in the plain strain MD simulation an atomically sharp rigid indenter is coming into contact with an ideally flat substrate. The substrate material is considered to be Titanium with Young's modulus $E = 116GPa$ and Poisson's ratio $\nu = 0.36$. The dimensions of the whole model problem (the CM domain and the MD patch embedded in it) are $2.02 \cdot 10^{-4} m \times 1.01 \cdot 10^{-4} m$. A domain of the model problem directly under the nanoindenter is calculated by the MD. The MD patch is of dimensions $1.16 \cdot 10^{-9} m \times 1.507 \cdot 10^{-8} m$.

The MD analysis is performed on constant temperature of $100^0 C$ by using the Nose-Hoover thermosetting method (as presented in [12]). The MD part of the substrate is approximated by two-dimensional triangular lattice, which is equivalent to three-dimensional continuum under the plane strain conditions [13]. On the other hand, on the CM domain simulation is three-dimensional.

The transition from two-dimensional MD phase of simulation to the three-dimensional CM phase of simulation is performed by mirroring input values of MD displacements along the third dimension (i.e., along the thickness).

Following equilibration, the intrusion of nano-indenter into the substrate takes place on the upper boundary of MD domain. It is important to emphasize that that this is an ongoing project, which renders a couple of simplifications necessary for the sake of the expedient code development. Specifically, the left and right boundaries of MD domain are free to deform, while the bottom boundary of MD domain is currently fixed. Also, the MD domain is admittedly miniscule at present— 41×61 atoms—although an order-of-magnitude larger MD ensembles are feasible on the PC used.

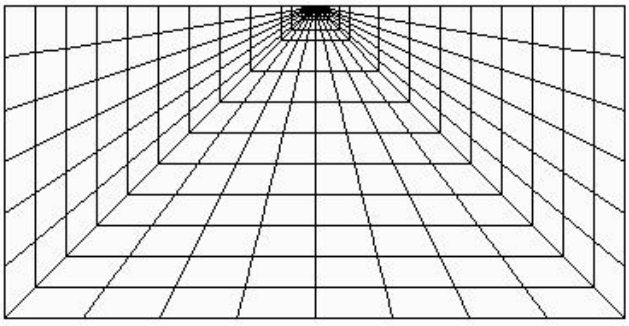

Fig. 4. Nanoidentation model problem

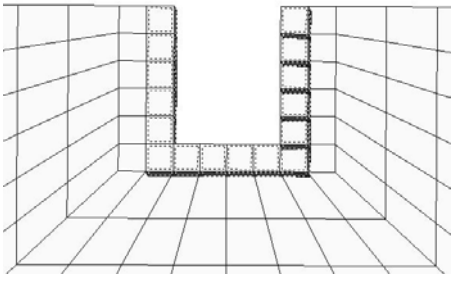

Fig. 5. Nanoidentation model magnified around MD domain

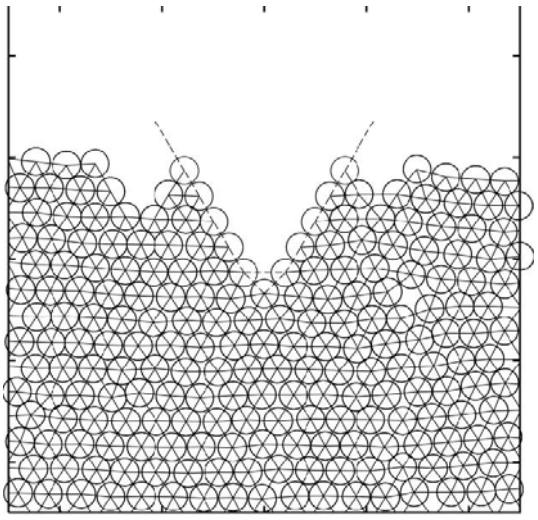

Fig. 6. Atomic configuration around indenter tip

At the onset of indentation, a dominant atomistic mechanism of plastic deformation is the local diffusional flow of the substrate atoms, resulting in their pile-up around the indenter tip ("wetting" of the tip). Subsequently, as the deformation energy accumulates around the tip, the edge dislocations are emitted from the tip region, as indicated in Fig. 7. The dislocations glide on their slip planes until they encounter the lateral (left and right) MD-region boundary, which results in formation of slip bands (slip discontinuities, dislocation steps). The formation of these bands is also captured by the localization of the deformation and stress fields of the CM region depicted in Figs. 7 and 8.

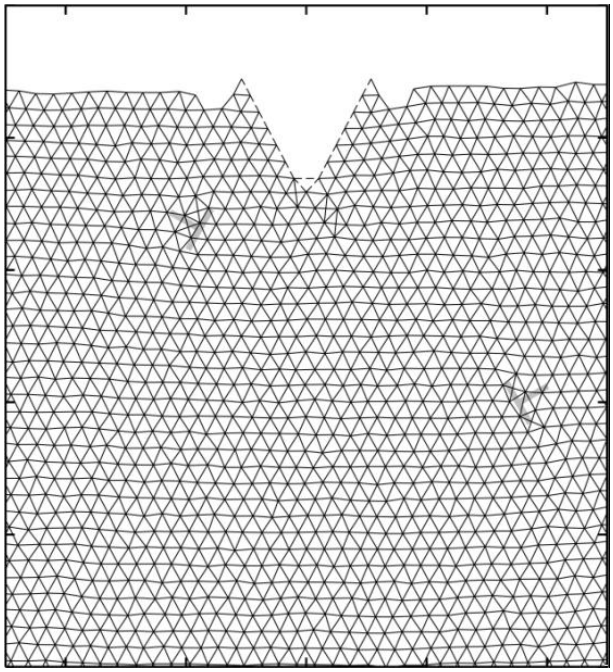

Fig. 7. Edge dislocations on slip planes

Thermal fluctuations in the MD part of the substrate around the prescribed temperature of $T = 100\,°C = 373\,K$ are presented in Fig. 8.

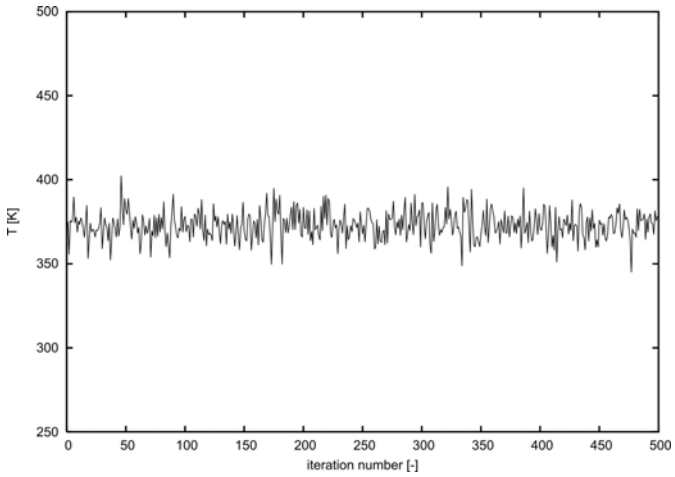

Fig. 8. Thermal fluctuations around prescribed temperature

As indicated before, the displacements are transferred from MD to CM domain by one-to-one correspondence between MD and CM domains. In the first incremental step, which is reported herein, the coordinates of bridging nodes and theirs displacements are given in Table 1.

From results obtained we may se that no spurious displacement occurs in the finite element model. In addition, resulting nonuniform stress t^{yy} field is direct consequence of the prescribed displacements on the boundary that change sign (see Table 1) and that are nonsymmetrical. Obtained results of this preliminary multiscale analysis, are affirmative for future research.

Atom No.	x	y	u_x	u_y
0	-57.3E-10	0.0	-4.674E-10	-8.678E-10
492	-57.3E-10	-30.1E-10	-5.503E-10	-8.813E-10
984	-57.3E-10	-60.3E-10	-5.589E-10	-9.607E-10
1476	-57.3E-10	-90.4E-10	-6.453E-10	-1.033E-9
1968	-57.3E-10	-120.6E-10	-4.804E-10	-8.307E-10
2460	-57.3E-10	-150.7E-10	-1.003E-10	-2.948E-10
40	58.7E-10	0.0	4.122E-10	-1.035E-9
532	58.7E-10	-30.1E-10	5.499E-10	-1.091E-9
1024	58.7E-10	-60.3E-10	5.304E-10	-1.109E-9
1516	58.7E-10	-90.4E-10	5.345E-10	-1.037E-9
2008	58.7 E-10	-120.6E-10	2.129E-10	-6.304E-10
2500	58.7 E-10	-150.7E-10	-3.051E-11	-4.398E-10

Table 1. Nanoidentation: coordinates and displacements on boundaries of MD domain (left and right)

First incremental step in our numerical example give us the displacement $[m]$ and stress field $\left[N/m^2\right]$ shown in Fig. 9, 10 and 11, respectively.

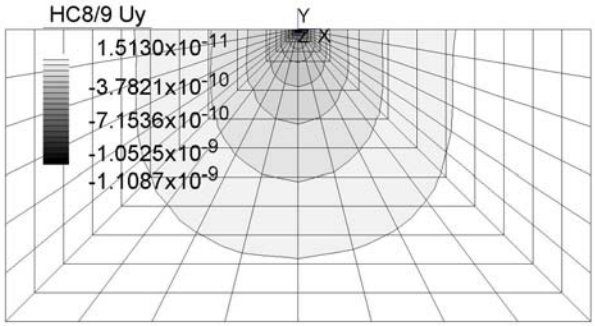

Fig. 9. Nanoidentation model: displacement field u_y after first increment of analysis of the whole model

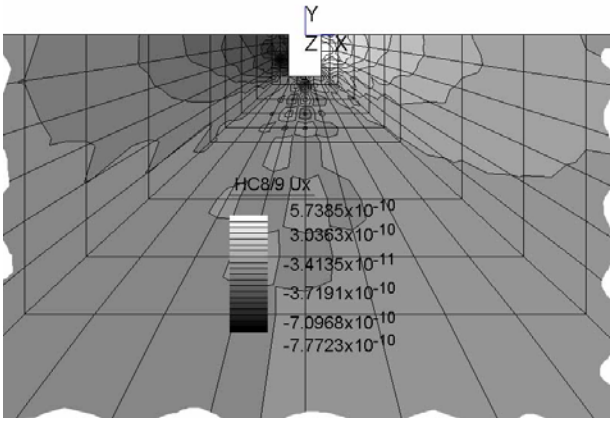

Fig. 10. Nanoidentation modelČ displacement field u_x after first increment of analysis in CM region neararound MD region after first increment of analysis

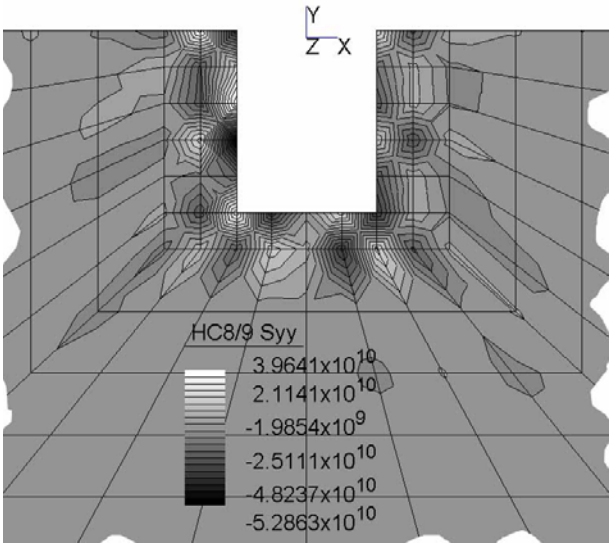

Fig. 11. Nanoidentation model: stress field in CM region neararound MD region after first increment of analysis

CONCLUSION

The present paper introduces a three-dimensional multiscale approach to thermo-mechanical analysis of a crystalline lattice with defects (the MD method), embedded in a large CM domain (the finite element method). This approach has been arousing perennial interest in the research community since it offers advantage of deeper understanding of the underlining physical phenomena facilitated by the molecular mechanics with the computational expediency of the finite element method; an appropriate computational technique is used for each scale.

It is shown that present approach based on direct linking, that is one-to-one correspondence, between molecular dynamics on atomistic scale and primal-mixed finite element scheme on macroscale, is reliable and efficient.

Finally, it cannot be overemphasized that this is an ongoing project; future work will address current oversimplifications and shortcomings.

REFERENCES

[1] Lawn, B (1993) Fracture of Brittle Solids. Cambridge University Press.

[2] Belytschko, T. and Xiao S.P. (2003) Coupling Methods for Continuum Model with Molecular Model. International Journal for Multiscale Computational Engineering 1 (1): 115-126.

[3] Mijuca D (2004) On hexahedral finite element HC8/27 in elasticity. Computational Mechanics 33 (6): 466-480

[4] Holian BL, Voter AF, Wagner NJ, Ravelo RJ, Chen SP, Hoover WG, Hoover CG, Hammerberg JE, and Dontje TD (1991) Effects of pairwise versus many-body forces on high-stress plastic deformation. Phys. Rev. A 43 (6): 2655-2661.

[5] Ghoniemy NM,Esteban P. Busso EP, Kioussis N,Huang H (2003) Multiscale modelling of nanomechanics and micromechanics: an overview, Phil. Mag., 83:3475-3528.

[6] Rao S, Hernandez C, Simmons,JP, ParthasarathyTA., Woodward C (1998) Phil. Mag. A77, 231

[7] Bathe KJ (2001) The inf-sup condition and its evaluation for mixed finite element methods. Computers & Structures, 79: 243-252

[8] Ortiz M, Phillips R (1999), Adv. appl. Mech., 36, 1

[9] Duff IS, Gould NI, Reid JK, Scott JA, and Turner K (1991) Factorization of sparse symmetric indefinite matrices, IMA J. Numer. Anal., 11: 181-204

[10] Lu S, Dong M. (2003) An advanced bem for thermal and stress analyses of components with thermal barrier coating, Electronic Journal of Boundary Elements, 1: 302-315

[11] Holian BL and Ravelo R (1995) Fracture simulations using large-scale molecular dynamics, Phys. Rev. B 51 (17): 11275-11288.

[12] Holian BL, Voter AF, and Ravelo R. (1995) Thermostatted molecular dynamics: How to avoid the Toda deamon hidden in Nose-Hoover dynamics, Phys. Rev. E 52 (3): 2338-2347.

[13] Monette L and Anderson MP (1994) Elastic and fracture properties of the two-dimensional triangular and square lattices, Modelling Simul.Mater. Sci. Eng. 2: 53-66.